Immunity, Vol. 14, 81–92, January, 2001, Copyright ©2001 by Cell Press

Two Different, Highly Exposed, Bulged Structures for an Unusually Long Peptide Bound to Rat MHC Class I RT1-A^a

Jeffrey A. Speir,* James Stevens,†§ Etienne Joly,†‖ Geoffrey W. Butcher,†‡ and Ian A. Wilson*‡

*Department of Molecular Biology and Skaggs Institute for Chemical Biology
The Scripps Research Institute
10550 North Torrey Pines Road
La Jolla, California 92037

†Molecular Immunology Programme
The Babraham Institute
Cambridge CB2 4AT
United Kingdom

Summary

The rat MHC class Ia molecule RT1-A^a has the unusual capacity to bind long peptides ending in arginine, such as MTF-E, a thirteen-residue, maternally transmitted minor histocompatibility antigen. The antigenic structure of MTF-E was unpredictable due to its extraordinary length and two arginines that could serve as potential anchor residues. The crystal structure of RT1-A^a-MTF-E at 2.55 Å shows that both peptide termini are anchored, as in other class I molecules, but the central residues in two independent pMHC complexes adopt completely different bulged conformations based on local environment. The MTF-E epitope is fully exposed within the putative T cell receptor (TCR) footprint. The flexibility demonstrated by the MTF-E structures illustrates how different TCRs may be raised against chemically identical, but structurally dissimilar, pMHC complexes.

Introduction

In the laboratory rat, *R. norvegicus*, the intracellular assembly rate and antigenic properties of MHC class Ia molecule RT1-A^a depend on a functional dimorphism of the rat MHC-linked peptide transporter, TAP (Livingstone et al., 1989; Powis et al., 1992). TAP transports peptide fragments of intracellularly processed protein antigens into the endoplasmic reticulum for loading onto MHC class I molecules. RT1-A^a selectively binds peptides with Gln, Met, or Leu at position 2 (P2), Phe at P3, Pro at P4, and Arg at the C terminus (Powis et al., 1996; Stevens et al., 1998a). The two allelic forms of rat TAP (TAP-A and TAP-B) have different specificities for the C-terminal residue of the peptide: the TAP-A form, like human TAP, transports peptides bearing a variety of C-terminal residues, whereas TAP-B, like mouse TAP, is far more selective for hydrophobic C-terminal residues (Momburg et al., 1994). An analysis of laboratory rat strains (Joly et al., 1998) revealed that *RT1* haplotypes expressing TAP-A encode some MHC class Ia molecules, such as RT1-A^a, which bind peptides with basic C termini, possibly by utilizing a triad of acidic residues rarely found within the peptide binding groove (Powis et al., 1996). By contrast, class Ia molecules in rat strains with the more restrictive TAP-B transporter select for hydrophobic or aromatic peptide C termini (Stevens et al., 1998a, 2000a). The roughly 20-fold slower assembly rate of RT1-A^a, when associated with homozygous *TAP-B*, was explained by the strong preference of RT1-A^a for C-terminal arginine in its peptide anchor motif (Powis et al., 1996). These findings suggest coevolution of the rat TAP transporter and genetically associated class Ia alleles (Joly and Butcher, 1998; Joly et al., 1998).

We have embarked on studies to examine structural differences between rat class Ia molecules from both the *TAP-A* and the *TAP-B* groups, starting with RT1-A^a bound to a natural ligand, MTF-E. MTF-E is a thirteen-residue peptide (ILFPSSERLISNR) derived from mitochondrial ATPase6 (residues 29–41), which corresponds to the CTL epitope defining a rat minor histocompatibility antigen ([miHA]; Davies et al., 1991; Bhuyan et al., 1997). The sequence of the MTF-E peptide, which carries arginine both at its C terminus and at an internal position, led to uncertainty as to which of the two arginine side chains might act as an anchor residue and how RT1-A^a can efficiently bind peptides up to 15 residues in length (Stevens et al., 1998b).

Class I MHC-bound peptides that are longer than 8–10 residues have not been characterized structurally, so their peptide binding mode, conformation, and recognition by T cells is unknown. Crystal structures of class I molecules binding 9–10 residue peptides have so far demonstrated two options for binding slightly longer peptides: (1) conventional binding of both the peptide N and C termini at the ends of the groove leaving the central residues to bulge or "zig-zag" through the groove to accommodate extra amino acids "inserted" between anchor residues (Fremont et al., 1992; Madden et al., 1993; Achour et al., 1998; Li et al., 1998); or (2) extension of the peptide C terminus through a hole created by structural rearrangement of MHC side chains so that the peptide can overhang the binding groove (Collins et al., 1994).

We have determined the crystal structure of RT1-A^a-MTF-E to 2.55 Å resolution to elucidate the register of MTF-E bound to RT1-A^a, to examine the detailed interactions between the anchored arginine side chain and the proposed F pocket acidic triad, and to resolve the conformation of MTF-E responsible for presenting the miHA epitope to T cells.

Results

RT1-A^a Structure

The crystal structure of the RT1-A^a-MTF-E complex was determined by molecular replacement to 2.55 Å resolution (Experimental Procedures, Table 1). The final model

‡To whom correspondence should be addressed (e-mail: geoff.butcher@bbsrc.ac.uk [G. W. B.], wilson@scripps.edu [I. A. W.]).
§Present address: Department of Molecular Biology and Skaggs Institute for Chemical Biology, The Scripps Research Institute, 10550 North Torrey Pines Road, La Jolla, California 92037.
‖Present address: UPCM, CNRS UPS 2163, CHU Purpan, 31300 Toulouse, France.

Table 1. X-ray Data Processing and Refinement Statistics for the RT1-A^a-MTF-E Complexes

	Data Processing		
Resolution range (Å)	20–2.55	20–5.46	2.64–2.55
Unique reflections	28993	3071	2757
Completeness (%)	94.3	94.1	91.2
Completeness $I/\sigma_I>3$ (%)	66.4	86.9	31.6
R_{merge} (%)[1]	9.5	4.1	31.8
Average I/σ_I	11.4	30.6	2.6
Redundancy[2]	3.2	3.6	2.7
	Refinement[3]		
Resolution range (Å)	20–2.55	2.64–2.55	
R_{cryst}[4] (number of refls)	0.224 (26801)	0.319 (2414)	
R_{free}[4] (number of refls)	0.284 (2177)	0.370 (197)	
Number of atoms[5] (C^α atoms)	6559 (774)		
Water molecules: 139	Mol A real space CC[7]: 0.91		
Coordinate error[6]: 0.42 Å	Mol B real space CC[7]: 0.90		
Protein Geometry and Thermal Parameters			
Rms Deviation from ideality		Ramachandran Plot	
bonds	0.007 Å	favored	87.6%
angles	1.4°	allowed	11.8%
dihedrals	25.3°	generous	0.6%
impropers	0.9°	disallowed	0%
	Average B Values (Å^2)		
Mol A		Mol B	
all atoms	26	all atoms	28
heavy chain	25	heavy chain	29
β_2m	30	β_2m	23
peptide	15	peptide	39
	waters 24		

Data given are for molecules A and B combined unless otherwise noted. The space group is $P2_12_12_1$ with two molecules per asymmetric unit. The unit cell dimensions are a = 86.9 Å, b = 90.7 Å, c = 117.4 Å.

[1] $R_{merge} = (\Sigma_h\Sigma_i|I_{hi}-<I_h>|/\Sigma_h\Sigma_i I_{hi}) \times 100$ where $<I_h>$ is the mean of the I_{hi} observations of reflection h.

[2] Redundancy = < # of observations / # of unique reflections >.

[3] Statistics for all data with $F/\sigma_F \geq 0$.

[4] $R_{cryst} = (\Sigma_h|F_o-F_c|/\Sigma_h F_o)$ where F_o and F_c are the observed and calculated structure factors: R_{free} is R_{cryst} computed with only the test set structure factors.

[5] Number for all non-hydrogen atoms, including waters.

[6] Estimated from cross-validated Luzzati plots (Luzzati, 1952) using a low-resolution limit of 5 Å.

[7] Correlation coefficient (CC) computed with program O (Jones et al., 1991) for all protein atoms in CNS σ_A-weighted $2F_o$-F_c maps.

consists of two RT1-A^a-MTF-E complexes (labeled A and B) in the crystal asymmetric unit and 139 water molecules (R_{cryst} = 22.4%, R_{free} = 28.4%). The heavy chain (residues 1–275) and β_2-microglobulin (β_2m, residues 1–99) polypeptides in both complexes adopt the standard MHC class I and immunoglobulin-like folds (Madden, 1995). The main chain atomic positions in core residues of the individual $\alpha_1\alpha_2$ (residues 1–181), α_3 (residues 182–275), and β_2m domains were tightly restrained between molecules A (molA) and B (molB) during refinement (rmsd of 0.04 Å); however, superposition of all their equivalent Cα atoms results in rmsd values of 0.53 Å, 0.33 Å, and 0.50 Å, respectively, due to considerable differences in some loop structures. Broader restraints were not implemented due to an approximate 7° rotation between the α_3 and β_2m domains of molB relative to molA (when the $\alpha_1\alpha_2$ domains are aligned) that is a consequence of crystal packing. The overall quaternary structures of the RT1-A^a heterodimers are closely similar to published crystal structures of both human and mouse MHC class Ia molecules (rmsd of 0.86–1.65 Å for all Cα atoms).

Individual peptide binding by MHC class I is sequence dependent and requires residues often located at or near the peptide termini (anchor residues) to match the polymorphism and physicochemical properties of allele-specific MHC binding pockets (A–F starting from the peptide N terminus; reviewed by Madden, 1995). The RT1-A^a peptide binding groove displays some novel features while still maintaining the basic A-F pocket substructure. The surface area of the RT1-A^a groove (660 Å^2) is slightly smaller than in most other class Ia molecules ($\geq$ 700 Å^2; Figure 1), due largely to a prominent ridge at its midsection composed of Tyr152, Trp70, and Tyr9, which roughly separates the groove into two halves (Figures 1, 2A, and 2B). Interestingly, Trp70 is found exclusively in RT1-A^a among rat class I molecules and occurs in only 33 of the 1724 MHC class I molecules listed in the Pfam database (Bateman et al., 2000). Indeed, the Tyr152-Trp70 pairing is found only in RT1-A^a. Prominent ridges are also formed in the grooves of mouse class Ia molecules H2-L^d and H2-D^b by the clustering of Trp73, Trp147, and large side chains at position 97 but are located closer to the F pocket (Figures 1 and 2D; Young et al., 1994; Speir et al., 1998). Ridges that protrude to the same extent from the floor of the peptide binding

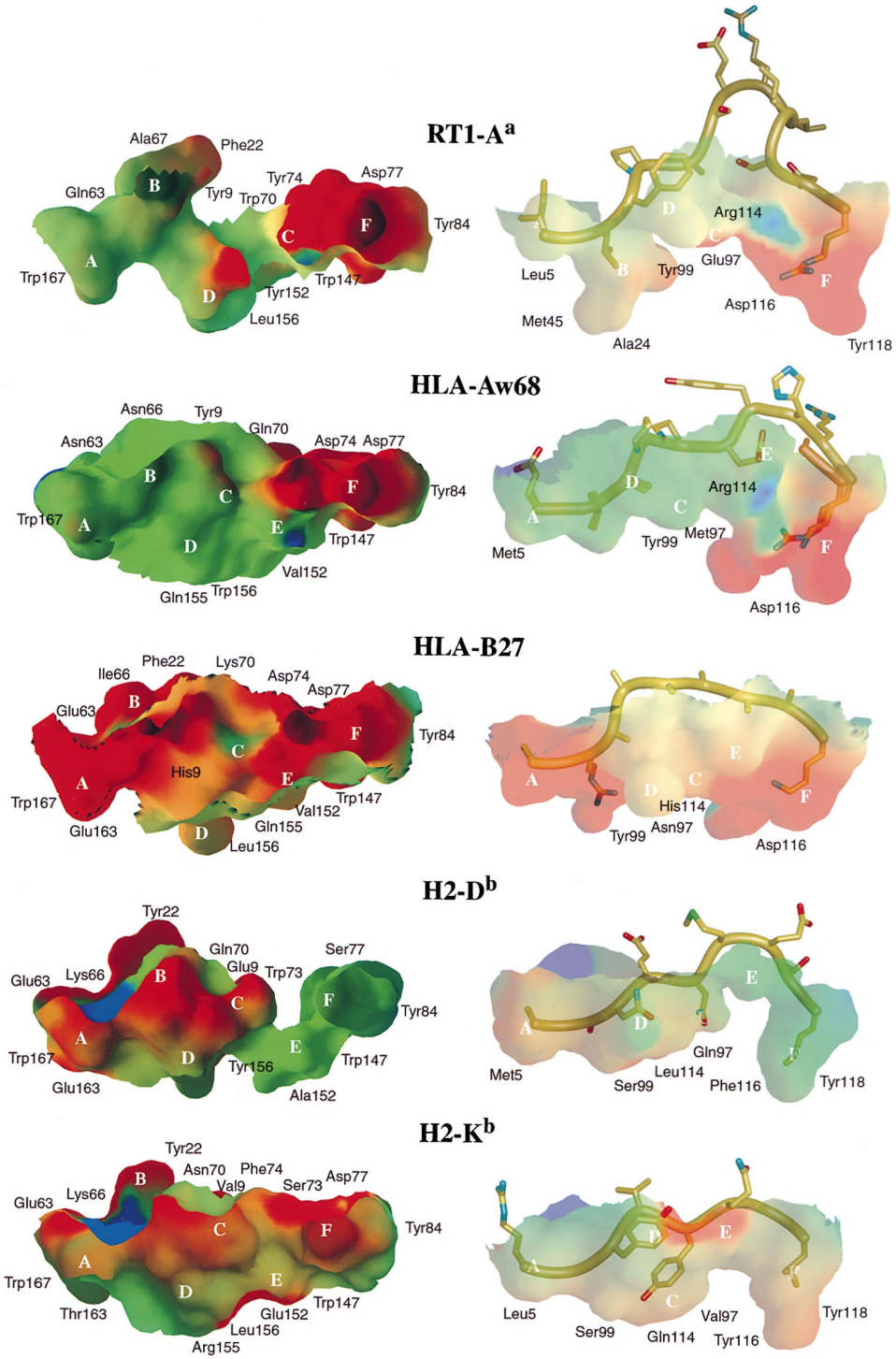

Figure 1. Comparative Anatomy of Five Class I MHC Peptide Binding Grooves

The cutaway molecular surfaces of the peptide binding grooves are shown with electrostatic potentials mapped to their surface. Positive potential (≥15 mV) is colored blue, neutral potential (0 mV) is colored green, and negative potential (≤−10 mV) is colored red. The colors become darker with increasing depth. Images on the left are views down into the MHC binding groove (α_1 helix on top). On the right are semitransparent side views of the same surfaces with bound peptides (N terminus on left) colored by atom type (yellow, carbon; red, oxygen; and blue, nitrogen). Allele-specific pockets are labeled A to F (white), but RT1-A[a] does not have a well-defined E pocket. Residues making a significant contribution to surface structure or chemistry are labeled at their location. The peptides displayed are MTF-E (molB) for RT1-A[a]; N- and C-terminal fragment structures (Cα atoms colored orange) determined from a peptide mixture (Guo et al., 1992) superimposed with the complete structure of a synthetic peptide (Collins et al., 1995) for Aw68; polyalanine structure (Madden et al., 1992) with modeled anchor residues (Rognan et al., 1994) for B27; influenza nucleoprotein 366–374 structure for D[b] (Infl-NP, Young et al., 1994); and vesicular stomatitis virus 52–59 structure for K[b] (VSV-8, Fremont et al., 1992). The groove molecular surfaces were scribed and their surface areas calculated using program GRASP (Nicholls et al., 1991) following the method of Segelke (Zeng et al., 1997).

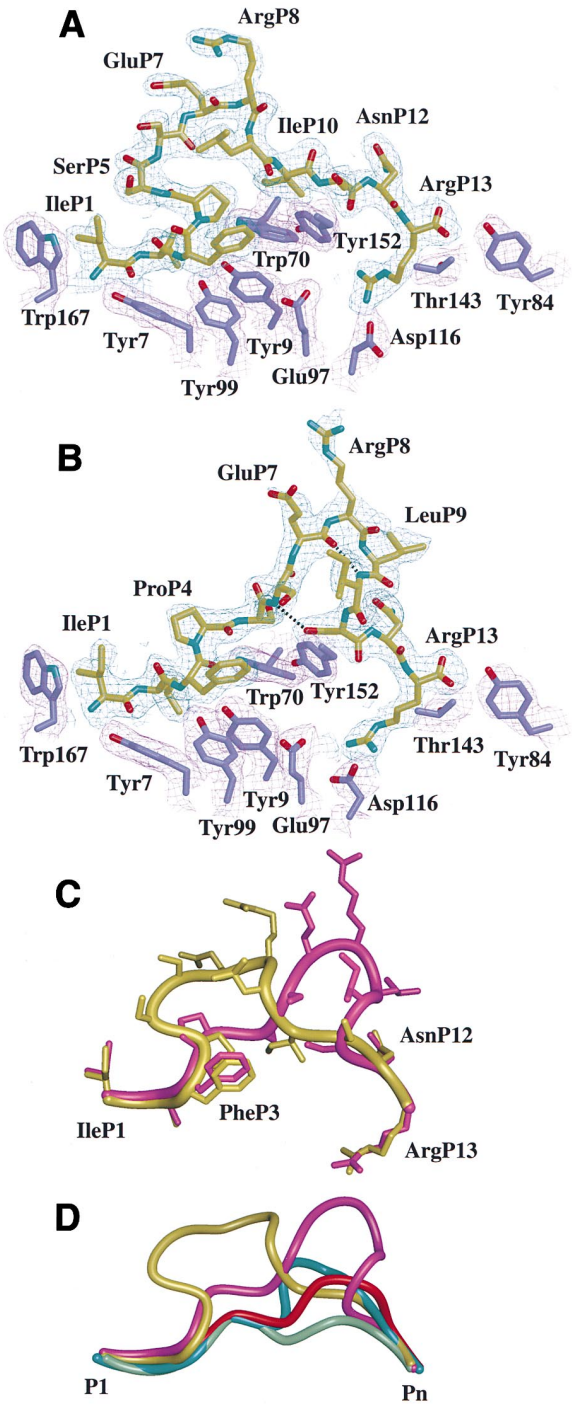

Figure 2. MTF-E Peptide Electron Density and Structure in the RT1-A^a Binding Groove

The final σ_A-weighted $2F_o$-F_c electron density (light blue) contoured at 1σ for the MTF-E peptide (ILFPSSERLISNR) and selected residues of the RT1-A^a peptide binding groove (dark blue) in molecules A (A) and B (B) are displayed, fitted with the refined model of RT1-A^a-MTF-E colored by atom type. A 2.0 Å cover radius has been applied to the density. Intrachain hydrogen bonds are shown as dotted black lines. (C) Comparison of the two MTF-E conformations from molecules A (yellow) and B (magenta). Superposition is the result of aligning only the Cα atoms of the RT1-A^a $\alpha_1\alpha_2$ domains. (D) Comparison of the four different peptide lengths (8, 9, 10, and 13 residues) observed in MHC class Ia crystal structures after superposition of their respective MHC $\alpha_1\alpha_2$ domains. Only traces of the peptide Cα atoms are shown for clarity. The two MTF-E conformations are shown as in (C) along with peptides from vesicular stomatitis virus 52–59 (green, 8 residues) bound to H2-K^b (Fremont et al., 1992), influenza nucleoprotein 366–374 (red, 9 residues) bound to H2-D^b (Young et al., 1994), and HIV gp120 P18-I10 (blue, 10 residues) bound to H2-D^d (Achour et al., 1998; Li et al., 1998). Nine residue peptides bound to H2-L^d (Balendiran et al., 1997; Speir et al., 1998) will have similar bulged conformations to that in H2-D^b.

groove are not present in other published MHC class I structures, such as H2-K^b, HLA-Aw68, and HLA-B27 (Figure 1).

The structural and chemical characteristics of the RT1-A^a pockets correlate well with the known anchor motif (Powis et al., 1996; Stevens et al., 1998a). The mostly hydrophobic B pocket is well suited for preferred P2 anchor residues Gln, Met, or Leu (Figure 1). Glutamine at P2 can reach both Tyr9 and main chain carbonyl oxygens within the B pocket to satisfy its hydrogen bonding potential. Similarly, the strong preference for phenylalanine at P3 is explained by the complementary hydrophobic character of the D pocket. In contrast, no pocket appears responsible for the preference of proline at P4. Instead, the ridge formed by Tyr152, Trp70, and Tyr9 is located where P4 or P5 would sit in an extended polypeptide chain (Figures 2A and 2B). The severely restricted phi angle of ProP4 may account for its frequency by promoting stable peptide conformations that are able to overcome the ridge and bind to RT1-A^a. A similar role for conserved prolines near the N termini of H2-L^d bound peptides has been suggested previously (Speir et al., 1999).

Thirteen residues contribute to the large F pocket, but the acidic triad composed of Asp77, Glu97, and Asp116 clearly dominates the local electrostatic potential. Arg114 lies at the periphery of the pocket but is not able to counterbalance Glu97 and Asp116, which are in close proximity (Figure 1). The striking negative potential and depth of the F pocket are ideal for binding arginine, the strongly favored peptide C-terminal anchor residue (Powis et al., 1996; Stevens et al., 1998a). Human MHC molecules HLA-Aw68 and HLA-B27 have acidic F pockets that also select for basic peptide C termini (Figure 1; Guo et al., 1992; Madden et al., 1992). No mouse MHC class I molecule has been shown to require a basic C-terminal anchor, which is consistent with their largely hydrophobic F pockets (e.g., H2-L^d and H2-D^b, Figure 1).

MTF-E Peptide Structure

The MTF-E peptide adopts two completely different conformations in molecules A and B (rmsd for peptide main chain of 3.3 Å). Except for the P7-P8 side chains in molB, electron density for MTF-E was surprisingly continuous given the extent to which the peptide protrudes from the MHC surface (Figures 2A and 2B). The IleP1 and ArgP13 termini anchor the peptide in the groove such that the remaining eleven residues adopt highly exposed secondary structures composed of multiple β turns.

The peptide A (pepA) conformation consists of two consecutive (i, i+2) double turns (Hutchinson and

Table 2. Hydrogen Bonds and Salt Bridges between Peptide MTF-E and RT1-A[a]

Molecule A				Molecule B[1]			
Peptide			MHC[2]	Peptide			MHC[2]
IleP1	O	OH	Tyr159	IleP1	O	OH	Tyr159
LeuP2	N	OE1	Gln63	LeuP2	N	OE1	Gln63
	O	O Wat15-Gln63	NE2	PheP3	N	OH	Tyr99
PheP3	N	OH	Tyr99		O	NE1	Trp70
		O Wat68-Tyr9	OH	ProP4	O	NH2	Arg155
		O Wat68-Trp70	NE1			O Wat130-Arg155	NH2
		O Wat68-Try99	OH	SerP5	N	O Wat136-Ile66	O
ProP4	O	O Wat15-Gln63	NE2			O Wat136-Glu69	OE1
SerP5	N	O Wat47-Thr163	OG1		OG	O Wat136-Ile66	O
SerP6	O	O Wat50-Glu69	OE1			O Wat136-Glu69	OE1
GluP7	OE1	NE*	Arg65	SerP6	N	OG	SerP11
		NH1*	Arg65			O Wat130-Arg155	NH2
		O Wat73-Glu69	OE1		OG	NE	Arg155
	OE2	NH1*	Arg65			O Wat130-Arg155	NH2
ArgP8	N	OE2	Glu69	GluP7	O	N	IleP10
LeuP9	N	O Wat50-Glu69	OE1	IleP10	O	NZ	Lys146
	O	NH1	Arg155	SerP11	O	O Wat131-Asp77	OD2
SerP11	OG	NH1	Arg155		OG	OH	Tyr152
	O	O Wat17-Asp77	OD2	AsnP12	O	NE1	Trp147
AsnP12	O	NE1	Trp147	ArgP13	N	OD1	Asp77
	ND2	OD1	Asp77		O	O Wat137-Asp77	OD1
ArgP13	N	OD1	Asp 77			O Wat137-Thr80	OG1
	O	NZ*	Lys146		OT	OH	Tyr84
		O Wat10-Asp77	OD1			OG1	Thr143
		O Wat10-Thr80	OG1		NE	OD2*	Asp77
	OT	OH	Tyr84		NH1	OD2*	Asp116
		OG1	Thr143		NH2	OE1*	Glu97
	NE	OD2*	Asp77			OD1*	Asp116
	NH1	OD1*	Asp116				
		O Wat74-Asp116	OD1				
		O Wat74-Arg114	NH1				
	NH2	OD2*	Asp77				
		CZ‡	Tyr74				

[1] There are two intrachain hydrogen bonds in pepB: SerP6-SerP11 and GluP7-IleP10.

[2] An asterisk denotes a possible salt-bridge formed with the peptide and a double dagger denotes an amino-aromatic hydrogen bond (CZ atom chosen arbitrarily). The distance and geometry criteria for hydrogen bonds are the defaults used in HBPLUS (McDonald and Thornton, 1994). When a hydrogen bond is made from the peptide to the MHC via a bridging water, all hydrogen bonds from the water to the MHC are listed (e.g., Wat68). Glu97 is just beyond the distance limit for a salt-bridge to ArgP13 in molA. Waters 131 and 133 are within hydrogen bonding distance of the ArgP13 side chain in molB but lack proper geometry for bond formation.

Thornton, 1994) from LeuP2-LeuP9 composed of three overlapping type IV β turns (LeuP2-SerP5, ProP4-GluP7, and SerP6-LeuP9; Figures 2A and 2C). The turns act to deflect the central peptide residues outward from the RT1-A[a] binding groove and expose 29% of the peptide surface, which is slightly greater than other MHC class I peptides (18%–28%). The remaining C-terminal residues (IleP10-ArgP13) adopt an extended β structure. In contrast to the more immediate upswing of the pepA N-terminal residues, IleP1-GluP7 of peptide B (pepB) form an extended β structure that gradually rises out of the RT1-A[a] peptide binding groove (Figures 2B and 2C). The C-terminal half of pepB is an (i, i+2) double turn that exposes 36% of the peptide surface beginning with a hydrogen-bonded type I′ β turn (GluP7-IleP10; Figure 2B; Table 2), and ending in a type I β turn (LeuP9-AsnP12) at the anchored C terminus. A second internal hydrogen bond between SerP6 and SerP11 may help to stabilize the overall double turn structure (Figure 2B; Table 2).

Crystal packing contacts greatly influence the conformation of pepA. Seven of the thirteen residues make over 50 interactions with a single, symmetry related molecule. The α_1 domain helix of the symmetry related protein sits over the pepA C terminus, perhaps stabilizing the series of β turns near the N terminus. Moreover, the average thermal factor (B value) for pepA (15 Å^2) is less than half that for pepB (39 Å^2, Table 1), consistent with a more static structure restricted by multiple contacts with nearby molecules. Peptide B has only eleven distant crystal packing contacts that are made with a single, symmetry related molecule.

The total exposed surface areas for peptides A and B (357 Å^2 and 449 Å^2, respectively) are the largest yet calculated for an unmodified class I peptide by more than 100 Å^2. Indeed, the exposed surface of pepB is 300 Å^2 larger than that of an eight-residue peptide (146 Å^2) bound to H2-K^b (Fremont et al., 1992; Figure 2D). Residues SerP5-ArgP8 in pepA and residues SerP6-IleP10 in pepB are the most exposed due to their location on the β turns reaching furthest from the groove (Figure 2C). Peptide B residues GluP7-ArgP8 actually protrude up to 15 Å above the MHC groove and are 100% accessible. Both conformations of MTF-E present

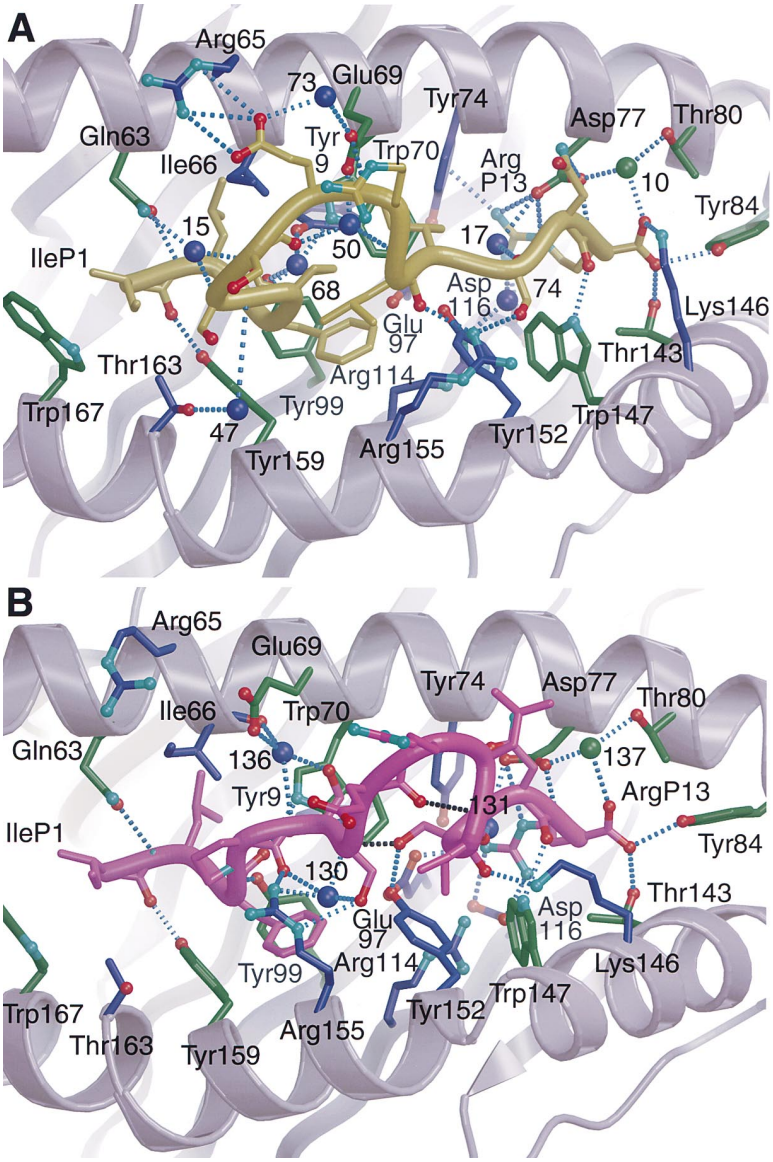

Figure 3. MTF-E Hydrogen Bonding in the RT1-A^a Binding Groove

The view is looking directly down into the peptide binding grooves (shown as gray ribbon diagrams) of molecules A (A) and B (B) with selected side chains and water molecules colored green, if they maintain closely similar contacts to MTF-E in both molecules, and colored blue, if they are dissimilar. Peptides are represented as in Figure 2C. Oxygen atoms are colored red and nitrogen atoms are colored cyan in both peptide and MHC molecules. Hydrogen bonds and salt bridges are shown as dotted lines.

substantially greater peptide binding surface for recognition by a TCR than previously observed in MHC crystal structures (Figure 2D).

MTF-E Interactions with RT1-A^a

Some 272 contacts are made between pepA and RT1-A^a, of which 32 are hydrogen bonds or salt bridges (Table 2). Nearly half of the hydrogen bonds (14) are mediated by eight bridging water molecules. Peptide B makes 58 fewer contacts (214) with RT1-A^a, but 29 are hydrogen bonds or salt bridges (Table 2). A third of these hydrogen bonds (10) are, in fact, made via only four bridging water molecules.

At their termini, both peptides are bound similarly by standard interactions previously observed in class I structures (reviewed by Madden, 1995). The greatest departure from conserved interactions in RT1-A^a occurs at the MTF-E C terminus. In other MHC class I structures, Lys146 often forms a salt bridge with the C-terminal carboxylate group, such as in molA. By contrast, Lys146 in molB forms a hydrogen bond with the IleP10 carbonyl oxygen positioned above the groove, forming the only polar interaction between the highly exposed pepB bulge and RT1-A^a (Figure 3).

Interactions of the central MTF-E residues with RT1-A^a vary considerably due to the different peptide conformations. A lack of any contacts between pepB GluP7-ArgP8 and RT1-A^a accounts for their 100% solvent exposure, and LeuP9 has only a single van der Waals contact with the side chain of Lys146. The same residues on pepA make 18 contacts (including three salt bridges) with Arg65, Ile66, Glu69, Tyr152, and Arg155 (Table 2; Figure 3). Arg155, like Lys146, forms distinctly different peptide contacts between molecules A and B (Table 2) in order to avoid steric clashes with LeuP9. Thus, the different peptide conformations are accommodated, in part, by conformational adjustments of more than ten MHC residues that line the RT1-A^a peptide binding groove (see blue residues in Figure 3).

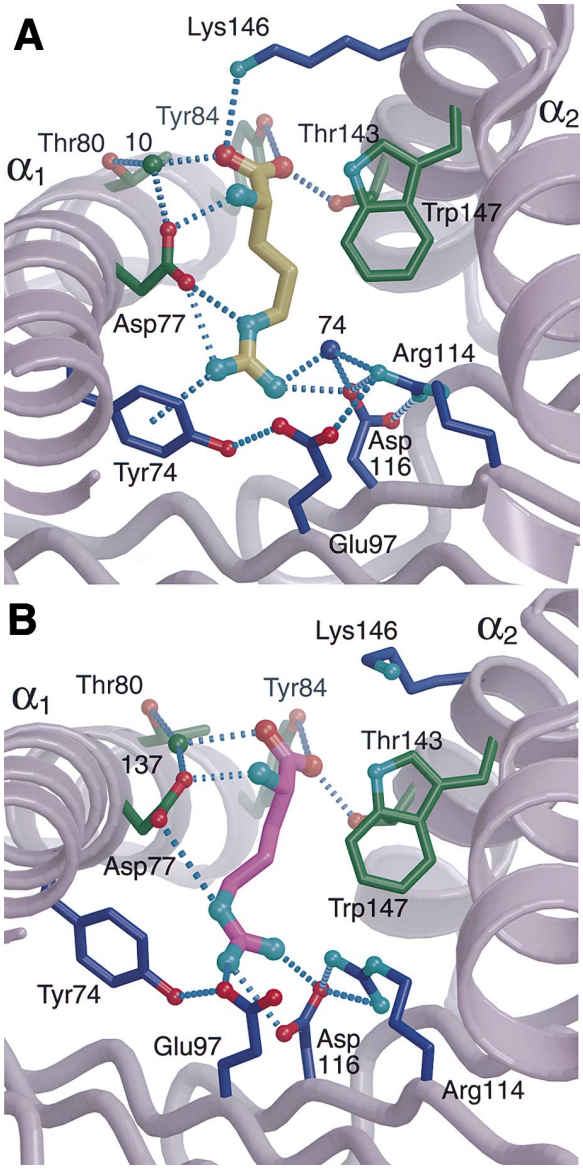

Figure 4. The Rat RT1-A^a F Pocket

Hydrogen bonds and salt bridges between ArgP13 and residues of RT1-A^a molecules A (A) and B (B) are shown as dotted lines. Coloring is the same as in Figure 3. The views are from inside the MHC binding groove looking toward the peptide C terminus.

In the F pocket of RT1-A^a, a triad of acidic residues at positions 77, 97 and 116, that nearly form the vertices of an isosceles triangle, surround the C-terminal ArgP13 guanidinium group and form an intricate hydrogen bonding network (Figure 4). No human or mouse class I MHC molecule has acidic residues at all three of these positions. Two slightly different conformations for the buried ArgP13 side chains are observed with at least four hydrogen bonds or salt bridges formed by each with RT1-A^a (Figures 4A and 4B; Table 2). While Asp116 switches between two rotamers, perhaps in coordination with the slightly different orientations of the ArgP13 side chains, the conformations of Asp77 and Glu97 are nearly identical. Asp77 forms an additional salt bridge to ArgP13 in molA because the guanidinium group tilts toward the α_1 helix, but the guanidinium group also moves slightly beyond the acceptable distance for a salt bridge with Glu97 (Figure 4A). The closer proximity to the α_1 helix also permits formation of a π-cation interaction (Dougherty, 1996) with Tyr74. A salt bridge with Asp77 and a hydrogen bond with Tyr74 in molA are exchanged for additional salt bridges with Glu97 and Asp116 in molB (Figure 4B).

Discussion

Structure of Long Peptides Bound to Class I MHC Molecules

With two exceptions, in which an additional glycine residue extends from the peptide C terminus (Collins et al., 1994) and where the peptide N terminus is shortened by one residue so that it cannot reach the A pocket (Khan et al., 2000), the reported structures of peptides bound to class Ia molecules have their N and C termini bound in the A and F pockets, respectively. The defined distance ($\sim$25 Å) from the A to F pockets most closely matches the length of a fully extended polypeptide chain of eight amino acids. Therefore, class I MHC bound peptides 9–10 amino acids in length must adopt bulged or meandering structures through the center of the binding groove (e.g., Figure 2D; Fremont et al., 1992; Madden et al., 1993; Achour et al., 1998; Li et al., 1998).

Identification of the rat MTF-E antigen raised the question of peptide register in the RT1-A^a binding groove (Bhuyan et al., 1997) and, hence, the number of peptide residues between the A and F pockets. RT1-A^a displays a strong preference for peptides with arginine at the C terminus (Powis et al., 1996; Stevens et al., 1998a). MTF-E has arginine at both the P8 and P13 positions, which suggested either a register with P9-P13 extended out of the MHC groove (e.g., as in Collins et al., 1994), or a considerable bulged conformation, depending on whether the first or second arginine is bound in the F pocket. A recent study on the binding of longer peptides to H2-K^b suggested that peptide extensions can be accommodated at the C terminus coincident with subtle pMHC conformational changes (Hörig et al., 1999). Nevertheless, a bulged peptide conformation was the favored prediction for MTF-E based on the lack of central anchor residues in the RT1-A^a peptide binding motif (Powis et al., 1996; Stevens et al., 1998a). The crystal structure of RT1-A^a-MTF-E revealed that ArgP13 is indeed bound in the F pocket and displayed two completely different bulged conformations for MTF-E that expose residues P5 to P10 to varying but substantial extents.

Interactions of RT1-A^a with the bulged, central peptide residues are dependent on the peptide conformation. Contacts between the central residues of peptide A and RT1-A^a appear to be facilitated by a conformation induced by crystal packing. Thus, the conformation of pepB is more likely to be representative of a solvent-exposed antigen. The MHC molecule adapts equally well to either peptide conformation with residue movements similar in magnitude to those observed in other class I molecules when comparing interactions of different peptides bound to the same MHC molecule (Fremont

et al., 1992; Madden et al., 1993). These adjustments are local and few in number leaving a uniform binding surface consistent with the role of the MHC molecule to present a myriad of different peptide sequences at the cell surface.

F Pocket Specificity for Basic Residues

Although RT1-A^a has a strong preference for arginine at the peptide C terminus, little to no signal for lysine is detected at the same position (Powis et al., 1996; Stevens et al., 1998a). Lysine may be disfavored because of its shorter side chain, which increases the distance to maintain contact with Asp116 and Glu97 in the F pocket (Thorpe et al., 1995). The RT1-A^a crystal structure confirms that ArgP13 of MTF-E forms salt bridges with Asp77, Asp116, and Glu97 (molB only), and explains the preference for arginine over lysine as the peptide C terminus. The triangular disposition of key acidic residues ensures multiple interactions with the side chain of arginine buried within the F pocket. Glu97 and Asp116 are positioned near the bottom of the pocket to form charged interactions with the guanidinium group and are within binding distance of Arg114. Arg114, found in all four of the rat MHC class I that have an identical F pocket acid triad (RT1-A^a, -A^f, -A1°, -A2°), constrains the orientation of Glu97 and Asp116 and may stabilize the deprotonated state of the buried carboxylic acids at physiological pH in the absence of bound peptide. Tyr74 also hydrogen bonds Glu97 in both molecules A and B, which may cement the position of the carboxylate in the F pocket. Arginine is able to form multiple defined hydrogen bonds in addition to electrostatic interactions with the F pocket creating a low free energy state that compensates for the entropic cost of restricting conformations of the contacting residues. The ammonium group of a lysine C terminus cannot form the same number of interactions, leaving unsatisfied bonding potential within the F pocket that can considerably reduce the stability of the pMHC complex (Dédier et al., 2000). Similarly, substitution of lysine for an arginine in a lysozyme antigen significantly affects antibody binding and results in over a 1000-fold reduction in affinity (Chacko et al., 1995). Thus, the position of Glu97 within the RT1-A^a F pocket creates a highly acidic environment with concentrated multivalent bonding potential best satisfied by peptides that end in arginine.

Supply and Demand of Longer Peptides

Although the peptide antigen processing pathway is optimized to produce and transport 8–10 residue peptides into the ER, longer peptides are supplied to class I molecules in at least small quantities (Bhuyan et al., 1997). RT1-A^a is genetically associated with rat TAP-A and benefits from the supply of peptides terminating in arginine actively transported by TAP-A into the ER. Interestingly, TAP-A appears to be able to transport longer peptides than TAP-B, although with reduced efficiency (Koopmann et al., 1996). TAP-B transports peptides more uniform in length consistent with the 9–12 residue peptide binding preferences of RT1-A1^u and RT1-A1^c, both TAP-B associated MHC molecules (Stevens et al., 1998b, 2000b). An intriguing possibility is that the class I RT1-A molecules actually evolved to function optimally with only one form of the transporter (Joly et al., 1998). Furthermore, the large central ridge formed by Tyr152, Trp70, and Tyr9 (Figures 1, 2A, and 2B) prohibits specific binding of central peptide residues in pockets, making RT1-A^a well suited to bind longer peptides supplied by TAP-A. Trp70 is present only in RT1-A^a among the thirteen cloned rat class I MHC, but the Tyr152-Tyr9 pairing is conserved in 5 of the 7 molecules associated with TAP-A compared to only 1 out of 6 TAP-B associated molecules (Joly et al., 1998). Essentially, Tyr152 paired with a bulky residue at either position 9 or 70 may be sufficient to create a formidable ridge for bound peptides to overcome. Thus, the ridge is strongly implicated in the poor association of peptides shorter than nine residues with RT1-A^a (Powis et al., 1996; Stevens et al., 1998b), since it would prevent MTF-E ArgP8 from reaching the F pocket, or conversely IleP1 from reaching the A pocket (Figure 2D). TAP-B, although ostensibly redundant, may be retained for its ability to deliver different and shorter peptides with appropriate C termini efficiently to the class I MHC molecules best able to present them to T cells (Joly and Butcher, 1998).

TCR Recognition of MTF-E and Flexible Epitopes

The consistent, approximately diagonal, footprint of the TCRs over the pMHC so far observed (reviewed by Garcia et al., 1999; Wilson, 1999), which places the TCR α and β chain hypervariable CDR3 loops in an ideal position between the MHC helices to examine the contents of the peptide binding groove, allows for more accurate prediction of the structural determinants of MHC-bound ligands that are likely to be responsible for T cell recognition. GluP7 of MTF-E is the key allelic residue defining this peptide fragment of mitochondrial ATPase6 as a miHA in rats. The allelic alternative to MTF-E has lysine at P7 and is poorly antigenic (Bhuyan et al., 1997). Both of the MTF-E conformations place GluP7 at the tip of the peptide bulges in the solvent exposed region above the helices of the MHC molecule and directly under the CDR3 hypervariable loops of the putative TCR footprint over RT1-A^a (Figures 5B, 5C, 5E, and 5F). Indeed, the exposed MTF-E residues clash with the CDR3 loops of the 2C, A6, and B7 TCRs after superimposing the MHC $\alpha_1\alpha_2$ domains in each TCR-pMHC crystal structure (Figure 5, Garboczi et al., 1996; Ding et al., 1998; Garcia et al., 1998). The majority of close contacts involving pepA are between residues P6-P8 and the CDR3α loops followed by a smaller number between P8-P10 and the CDR3β loops, whereas clashes with pepB residues P6-P10 primarily involve the CDR3β and 1β loops with a few close contacts also between P4-P7 and CDR3α (Figure 5).

The high elevation and exposure of epitope residues above the MHC binding groove require selection of T cells that can accommodate the large central bulges in longer peptides bound by RT1-A^a, or other MHC class Ia molecules with similar properties (Willcox et al., 1999). Interestingly, these two peptide conformations actually place their protruding bulges either in the "hot spot" between the TCR CDR3α and 3β loops seen for self- and foreign TCR-pMHC complexes (Degano et al., 2000) or next to the β chain CDRs, where increased or exclusive contacts to the peptide has been implicated as a

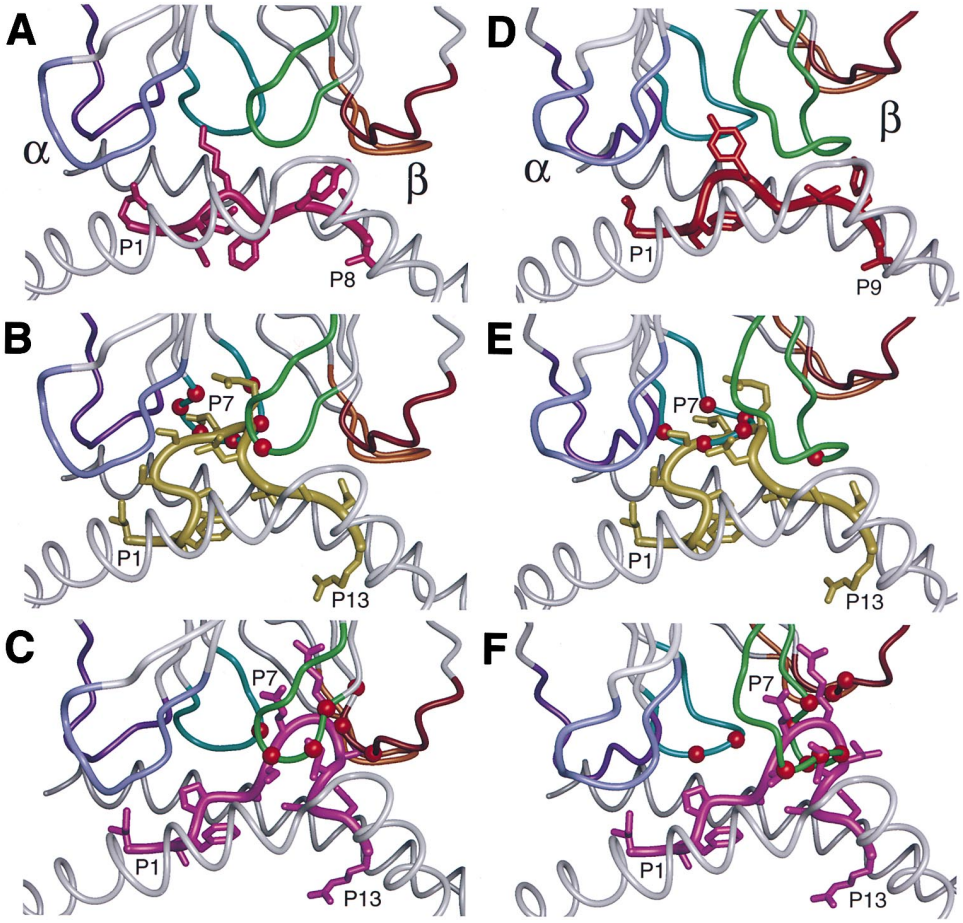

Figure 5. A Model of Potential TCR Interactions with RT1-A[a]-MTF-E

(A)–(C) show the interface of the 2C TCR (top) bound to natural ligand H2-K[b]-dEV8 (bottom) and fitted to MTF-E molecules A and B, respectively, by superimposing only the Cα atoms of the MHC $\alpha_1\alpha_2$ domains. (D)–(F) show the A6 TCR (top) bound to natural ligand HLA-A2-Tax (bottom) and fitted by the same method to MTF-E molecules A and B, respectively. Only Cα tracings of the TCR CDR loops and MHC α helices (gray) are shown for clarity. Large red spheres for TCR Cα atoms represent steric collisions between any main chain atoms of the TCR CDR loops and MTF-E peptides. The CDR loops are colored coded as follows: CDR3α, cyan; CDR2α, blue; CDR1α, purple; CDR3β, green; CDR2β, orange; and CDR1β, brown.

contributing factor in allorecognition (Speir et al., 1998, Figure 2D; Reiser et al., 2000). Either of these two scenarios for recognition of MTF-E is likely to require a deeper TCR combining site. Although the cavities in antibody combining sites actually tend to diminish with increasing antigen size (Wilson and Stanfield, 1993), the requirement for simultaneous interaction of the TCR CDR loops with both the peptide and MHC α helices dictates that peptide residues protruding from the MHC molecule must be accommodated within the TCR combining site. In addition, several residues located on the solvent-exposed regions of the $\alpha_1\alpha_2$ helices, and previously defined (or observed) as TCR contact residues (Bjorkman et al., 1987; Garboczi et al., 1996; Garcia et al., 1998), are found to have peptide-dependent conformations (e.g., Arg65, Glu69, Lys146, Arg155). Thus, potential changes to the TCR-pMHC interaction can result from the large size and different conformations of the MTF-E peptide and also from the indirect effect of peptide on MHC residues within the TCR footprint that can amplify the T cell response (e.g., Ghendler et al., 1998).

The different MTF-E structures raise two important questions: how flexible is MTF-E bound to RT1-A[a] and what effect does this flexibility have on TCR recognition? Changes in peptide configuration and cognate T cell recognition can result from anchor residue modification or mutation (Saito et al., 1999; Schmitt et al., 1999). T cells can also distinguish between unmodified pMHC molecules dependent upon whether peptide was processed internally or loaded on the outside of cells (Viner et al., 1996). Of course, the observed range of residue movement between peptide conformations A and B (up to 14 Å) may be extreme due to the effects of crystal packing. The unmolested bulge in pepB is stabilized by two intrachain hydrogen bonds (Table 2; Figure 2). Thus, the energetic cost of breaking two hydrogen bonds will limit the number of other conformations sampled but not prevent substantial movements. Nevertheless, any alternative conformations are likely to be closely related to the pepB structure.

Even larger conformational changes in MTF-E structure may also be possible through contact with the TCR.

The "flattened" structure of pepA caused by crystal contacts could be predictive of a structure adopted upon formation of the TCR-pMHC complex. Therefore, the fine structure of a pMHC complex having an unusually long peptide may vary considerably and, as a result, can change its antigenic identity. Unfortunately, T cell clones from the rat are not yet available to examine CDR length and sequence and to perform specific binding assays that could help resolve these important issues surrounding TCR recognition of substantially bulged peptides.

Thus, individual TCRs may recognize a particular MTF-E conformation that best complements clonotypic hot spots in the flexible combining site (e.g., Degano et al., 2000) or may use a more adaptive induced fit mechanism similar to antigen-induced rearrangements in antibody-antigen complexes (Wilson and Stanfield, 1994). In either case, TCR binding of MTF-E requires a modification of the present structural paradigm in pMHC recognition, consisting of reading out the features of an extended peptide largely buried between the MHC α helices, to include the incursion of highly exposed residues into the TCR combining site that will dramatically increase the contribution of peptide binding surface to complex formation (Figure 5). The crystal structure of an MHC-bound glycopeptide shows nearly equivalent exposure and greater potential flexibility for the synthetic glycan (Speir et al., 1999). Alterations in the structure of the TCR combining site or occupation of the large cavity between the α and β chains were also suggested for binding of the carbohydrate ligand. These compelling scenarios for T cell recognition of RT1-A^a-MTF-E and large glycopeptides are suitable for other unusually long peptides with their termini bound to class I molecules, since they will also form bulged structures that are exposed beyond the boundaries of the α helices that form the MHC groove.

Role of Longer Peptides Presented by Class I MHC

The full significance of class I MHC presentation of peptides longer than 8–10 residues remains unclear. An MHC class Ia allele able to accommodate a range of peptide lengths will theoretically find more peptides suitable for binding among a random set of sequences than a more length-sensitive allele. The amino acid composition of bulges in longer peptides is presumably less restrictive and would increase the diversity of sequences that can be presented to T cells (Guo et al., 1992). These potential benefits are balanced with the more unpredictable antigenic properties associated with longer peptides. The ability to shift between different conformations can create distinct multiple epitopes on a single peptide. The greater number of T cells able to bind a peptide that can display multiple epitopes increases the opportunity for harmful cross-reactivity, if the complete breadth of conformational isomers is not sampled in developing tolerance (Mason, 1998). The benefits offered by class I presentation of longer peptides, therefore, come at the cost of producing a special repertoire of tolerant T cells in order to prevent the destructive potential of multiple epitope display.

Experimental Procedures

Expression, Purification, and Crystallization of the RT1-A^a-MTF-E Complex

Rat β_2m and residues 1–276 of RT1-A^a were expressed in *Escherichia coli*, purified, and refolded with MTF-E peptide (ILFPSSERLISNR) as described previously (Stevens et al., 1998a). Centriprep 10 and Centricon 10 ultrafiltration units (Millipore, Bedford MA) were used to concentrate the complex to 15 mg/ml in 10 mM HEPES, 25 mM NaCl, and 1 mM EDTA (pH 7.2). Reproducible small crystals that diffracted to 2.55 Å resolution grew using sitting drop vapor diffusion at 17°C by mixing Hampton Crystal Screen II solution 26 (0.1 M MES, 0.2 M ammonium sulfate, and 15%–20% MPEG 5000) in a 1:1 ratio with protein solution in the droplet.

Data Collection and Processing

Diffraction data were collected at Stanford Synchrotron Radiation Laboratory (SSRL) beamline 9-1 (λ = 0.98 Å, 30 cm MAR image plate) with a small (0.1 × 0.1 × 0.05 mm), flash-cooled (93 K, 25% glycerol) single crystal. The data were indexed and integrated with the program DENZO (Otwinowski and Minor, 1997). The crystals are orthorhombic, $P2_12_12_1$, with unit cell dimensions a = 86.9 Å, b = 90.7 Å, and c = 117.4 Å. The V_m (Matthews, 1968) of 2.46 $Å^3$ Da^{-1} indicated two molecules per asymmetric unit with a solvent content of 50%. The data were merged, scaled, and reduced to a unique reflection set with SCALEPACK (Table 1; Otwinowski and Minor, 1997).

Molecular Replacement and Model Refinement

HLA-A2 coordinates (Collins et al., 1994) stripped of peptide provided the clearest molecular replacement solution (CC = 41.2, R = 0.44%) for both molecules in the asymmetric unit using AMoRe (Navaza, 1994). Molecules A and B are related by improper noncrystallographic symmetry consisting of a 101.9° rotation followed by a 38.4 Å translation along the rotation axis.

A random set of 7.5% of the reflections between 20 and 2.55 Å (Table 1) were excluded from refinement to monitor R_{free} (Brünger, 1997). Only procedures implemented in X-PLOR v3.851 (Brünger et al., 1987) or CNS v0.4 (Brünger et al., 1998) that minimized both R_{cryst} and R_{free} were utilized. The electron density of molecules A and B after rigid body refinement (R_{cryst} = 42.2%, R_{free} = 41.8%) showed distinct differences in peptide conformations, domain orientations, and side chain conformations. Density modification procedures were not used due to the already excellent electron density quality and concern that these procedures would obscure significant differences between molecules A and B. Noncrystallographic symmetry restraints of 300 kcal mol^{-1} $Å^2$ were applied only to the main chain atoms in the most similar regions of the individual MHC domains (e.g., loops and peptides excluded) as they gave the best refinement results as determined by R_{free} and electron density quality. The human β_2m molecule was replaced with the equivalent rat FcRn β_2m structure (Burmeister et al., 1994).

Several rounds of slow-cooled molecular dynamics (e.g., Kleywegt and Jones, 1997) and model building allowed the peptide to be unambiguously traced in both molecules (R_{cryst} = 25.8%, R_{free} = 32.9%). $3F_o$-$2F_c$, $2F_o$-F_c shake omit (McRee, 1993), and shaken, σ_A-weighted (Read, 1986) $2F_o$-F_c and F_o-F_c electron density maps were computed to reduce phase bias for model rebuilding. All residues of the RT1-A^a-MTF-E complex were built. The side chains of pepB residues GluP7 and ArgP8 are exposed, and their relatively high refined B values (48–67 $Å^2$) are reflective of their partial disorder. The final rounds of positional and B value refinement in CNS with 139 water molecules gave an R_{cryst} of 22.4% and an R_{free} of 28.4% (Table 1).

Structural Analysis and Illustrations

The RT1-A^a-MTF-E structure was compared with selected human and mouse class I TCR and pMHC complexes with PDB ID codes 2vaa, 2ckb, 1kbg, 1ao7, 1duz, 1hoc, 1bii, 1ddh, 1hsb, 1tmc, 1has, and 1roh (references given in text). Crystal structure analysis was performed with PROCHECK (Laskowski et al., 1993), PROMOTIF (Hutchinson and Thornton, 1996), CONTACSYM (Sheriff et al., 1987), BPLOT (Collaborative Computational Project 4, 1994), LSQKAB

(CCP4), CONTACT (CCP4), LSQMAN (Kleywegt, 1996), and HBPLUS (McDonald and Thornton, 1994). Buried surface areas were computed with MS (Connolly, 1983) using a 1.4 Å radius probe. Figures 2C, 2D, and 5 were created using MIDAS (Ferrin et al., 1988). Figures 2A, 2B, 3, and 4 were created using a combination of CNS, BOBSCRIPT (Esnouf, 1997), and Raster3D (Bacon and Anderson, 1988).

Acknowledgments

We thank Kirsten Fischer Lindahl for important contributions to the identification of MTF-E, Markus Rudolph and Robyn Stanfield for helpful discussions, Trish Horton for technical assistance, and the staff at SSRL beamline 9-1 for excellent support. This study was funded by National Institutes of Health grant CA58896 (I. A. W.), a postdoctoral fellowship from National Institutes of Health training grant MH19185 (J. A. S.), and the UK Biotechnology and Biological Sciences Research Council (Core Competitive Strategic Grant to G. W. B., Project Grant 202/BCI05257 and a Research Fellowship to E. J.). This is manuscript #13565-MB from The Scripps Research Institute.

Received November 9, 2000; revised December 12, 2000.

References

Achour, A., Persson, K., Harris, R.A., Sundback, J., Sentman, C.L., Lindqvist, Y., Schneider, G., and Karre, K. (1998). The crystal structure of H-2D^d MHC class I complexed with the HIV-1-derived peptide P18-I10 at 2.4 Å resolution: implications for T cell and NK cell recognition. Immunity *9*, 199–208.

Bacon, D.J., and Anderson, W.F. (1988). Raster3D. J. Mol. Graph. *6*, 219–220.

Balendiran, G.K., Solheim, J.C., Young, A.C., Hansen, T.H., Nathenson, S.G., and Sacchettini, J.C. (1997). The three-dimensional structure of an H-2L^d-peptide complex explains the unique interaction of L^d with β_2-microglobulin and peptide. Proc. Natl. Acad. Sci. USA *94*, 6880–6885.

Bateman, A., Birney, E., Durbin, R., Eddy, S.R., Howe, K.L., and Sonnhammer, E.L. (2000). The Pfam protein families database. Nucleic Acids Res. *28*, 263–266.

Bhuyan, P.K., Young, L.L., Fischer Lindahl, K., and Butcher, G.W. (1997). Identification of the rat maternally transmitted minor histocompatibility antigen. J. Immunol. *158*, 3753–3760.

Bjorkman, P.J., Saper, M.A., Samraoui, B., Bennett, W.S., Strominger, J.L., and Wiley, D.C. (1987). The foreign antigen binding site and T cell recognition regions of class I histocompatibility antigens. Nature *329*, 512–518.

Brünger, A.T. (1997). The free R value: a more objective statistic for crystallography. Methods Enzymol. *277*, 366–396.

Brünger, A.T., Kuriyan, J., and Karplus, M. (1987). Crystallographic *R* factor refinement by molecular dynamics. Science *235*, 458–460.

Brünger, A.T., Adams, P.D., Clore, G.M., DeLano, W.L., Gros, P., Grosse-Kunstleve, R.W., Jiang, J.-S., Kuszewski, J., Nilges, N., Pannu, N.S., Read, R.J., et al. (1998). Crystallography and NMR system (CNS): a new software system for macromolecular structure determination. Acta Crystallogr. D *54*, 905–921.

Burmeister, W.P., Gastinel, L.N., Simister, N.E., Blum, M.L., and Bjorkman, P.J. (1994). Crystal structure at 2.2 Å resolution of the MHC-related neonatal Fc receptor. Nature *372*, 336–343.

Chacko, S., Silverton, E., Kam-Morgan, L., Smith-Gill, S., Cohen, G., and Davies, D. (1995). Structure of an antibody-lysozyme complex: unexpected effect of conservative mutation. J. Mol. Biol. *245*, 261–274.

CCP4 (Collaborative Computational Project 4) (1994). The CCP4 suite: programs for protein crystallography. Acta Crystallogr. D *50*, 760–763.

Collins, E.J., Garboczi, D.N., and Wiley, D.C. (1994). Three-dimensional structure of a peptide extending from one end of a class I MHC binding site. Nature *371*, 626–629.

Collins, E.J., Garboczi, D.N., Karpusas, M.N., and Wiley, D.C. (1995). The three-dimensional structure of a class I major histocompatibility complex molecule missing the α3 domain of the heavy chain. Proc. Natl. Acad. Sci. USA *92*, 1218–1221.

Connolly, M.L. (1983). Solvent-accessible surfaces of proteins and nucleic acids. Science *221*, 709–713.

Davies, J.D., Wilson, D.H., Hermel, E., Fischer Lindahl, K., Butcher, G.W., and Wilson, D.B. (1991). Generation of T-cells with lytic specificity for atypical antigens. I. A mitochondrial antigen in the rat. J. Exp. Med. *173*, 823–832.

Dédier, S., Reinelt, S., Reitinger, T., Folkers, G., and Rognan, D. (2000). Thermodynamic stability of HLA-B*2705-peptide complexes. Effect of peptide and major histocompatibility complex protein mutations. J. Biol. Chem. *275*, 27055–27061.

Degano, M., Garcia, K.C., Apostolopoulos, V., Rudolph, M.G., Teyton, L., and Wilson, I.A. (2000). A functional hot spot for antigen recognition in a superagonist TCR/MHC complex. Immunity *12*, 251–261.

Ding, Y.H., Smith, K.J., Garboczi, D.N., Utz, U., Biddison, W.E., and Wiley, D.C. (1998). Two human T cell receptors bind in a similar diagonal mode to the HLA- A2/Tax peptide complex using different TCR amino acids. Immunity *8*, 403–411.

Dougherty, D.A. (1996). Cation-pi interactions in chemistry and biology: a new view of benzene, Phe, Tyr, and Trp. Science *271*, 163–168.

Esnouf, R.M. (1997). An extensively modified version of MOLSCRIPT that includes greatly enhanced coloring capabilities. J. Mol. Graph. Model. *15*, 132–134.

Ferrin, T.E., Huang, C.C., Jarvis, L.E., and Langridge, R. (1988). The MIDAS display system. J. Mol. Graph. *6*, 13–27.

Fremont, D.H., Matsumura, M., Stura, E.A., Peterson, P.A., and Wilson, I.A. (1992). Crystal structures of two viral peptides in complex with murine MHC class I H-2K^b. Science *257*, 919–927.

Garboczi, D.N., Ghosh, P., Utz, U., Fan, Q.R., Biddison, W.E., and Wiley, D.C. (1996). Structure of the complex between human T-cell receptor, viral peptide and HLA-A2. Nature *384*, 134–141.

Garcia, K.C., Degano, M., Pease, L.R., Huang, M., Peterson, P.A., Teyton, L., and Wilson, I.A. (1998). Structural basis of plasticity in T-cell receptor recognition of a self peptide-MHC antigen. Science *279*, 1166–1172.

Garcia, K.C., Teyton, L., and Wilson, I.A. (1999). Structural basis of T cell recognition. Annu. Rev. Immunol. *17*, 369–397.

Ghendler, Y., Teng, M.K., Liu, J.H., Witte, T., Liu, J., Kim, K.S., Kern, P., Chang, H.C., Wang, J.H., and Reinherz, E.L. (1998). Differential thymic selection outcomes stimulated by focal structural alteration in peptide/major histocompatibility complex ligands. Proc. Natl. Acad. Sci. USA *95*, 10061–10066.

Guo, H.C., Jardetzky, T.S., Garrett, T.P., Lane, W.S., Strominger, J.L., and Wiley, D.C. (1992). Different length peptides bind to HLA-Aw68 similarly at their ends but bulge out in the middle. Nature *360*, 364–366.

Hörig, H., Young, A.C.M., Papadopoulos, N.J., DiLorenzo, T.P., and Nathenson, S.G. (1999). Binding of longer peptides to the H-2K^b heterodimer is restricted to peptides extended at their C terminus: refinement of the inherent MHC class I peptide binding criteria. J. Immunol. *163*, 4434–4441.

Hutchinson, E.G., and Thornton, J.M. (1994). A revised set of potentials for β-turn formation in proteins. Protein Sci. *3*, 2207–2216.

Hutchinson, E.G., and Thornton, J.M. (1996). PROMOTIF-a program to identify and analyze structural motifs in proteins. Protein Sci. *5*, 212–220.

Joly, E., and Butcher, G.W. (1998). Why are there two rat TAPs? Immunol. Today *19*, 580–585.

Joly, E., LeRolle, A.F., González, A.L., Mehling, B., Stevens, J., Coadwell, W.J., Hünig, T., Howard, J.C., and Butcher, G.W. (1998). Co-evolution of rat TAP transporters and MHC class I RT1-A molecules. Curr. Biol. *8*, 169–172.

Jones, T.A., Cowan, S., Zou, J.Y., and Kjeldgaard, M. (1991). Improved methods for building protein models in electron density

maps and the location of errors in these models. Acta Crystallogr. A *47*, 110–119.

Khan, A.R., Baker, B.M., Ghosh, P., Biddison, W.E., and Wiley, D.C. (2000). The structure and stability of an HLA-A*0201/octameric tax peptide complex with an empty conserved peptide-N-terminal binding site. J. Immunol. *164*, 6398–6405.

Kleywegt, G.J. (1996). Use of non-crystallographic symmetry in protein structure refinement. Acta Crystallogr. D *52*, 842–857.

Kleywegt, G.J., and Jones, T.A. (1997). Model building and refinement practice. Methods Enzymol. *277*, 208–230.

Koopmann, J.O., Post, M., Neefjes, J.J., Hämmerling, G.J., and Momburg, F. (1996). Translocation of long peptides by transporters associated with antigen-processing (TAP). Eur. J. Immunol. *26*, 1720–1728.

Laskowski, R.A., MacArthur, M.W., Moss, D.S., and Thornton, J.M. (1993). PROCHECK: a program to check the stereochemical quality of protein structures. J. Appl. Cryst. *26*, 283–291.

Li, H., Natarajan, K., Malchiodi, E.L., Margulies, D.H., and Mariuzza, R.A. (1998). Three-dimensional structure of H-2D^{d} complexed with an immunodominant peptide from human immunodeficiency virus envelope glycoprotein 120. J. Mol. Biol. *283*, 179–191.

Livingstone, A.M., Powis, S.J., Diamond, A.G., Butcher, G.W., and Howard, J.C. (1989). A trans-acting major histocompatibility complex-linked gene whose alleles determine gain and loss changes in the antigenic structure of a classical class I molecule. J. Exp. Med. *170*, 777–795.

Luzzati, V. (1952). Traitement statistique des erreurs dans la determination des structures cristallines. Acta Crystallogr. *5*, 802–810.

Madden, D.R. (1995). The three-dimensional structure of peptide-MHC complexes. Annu. Rev. Immunol. *13*, 587–622.

Madden, D.R., Gorga, J.C., Strominger, J.L., and Wiley, D.C. (1992). The three-dimensional structure of HLA-B27 at 2.1 Å resolution suggests a general mechanism for tight peptide binding to MHC. Cell *70*, 1035–1048.

Madden, D.R., Garboczi, D.N., and Wiley, D.C. (1993). The antigenic identity of peptide-MHC complexes: a comparison of the conformations of five viral peptides presented by HLA-A2. Cell *75*, 693–708.

Mason, D. (1998). A very high level of crossreactivity is an essential feature of the T-cell receptor. Immunol. Today *19*, 395–404.

Matthews, B.W. (1968). Solvent content of protein crystals. J. Mol. Biol. *33*, 491–497.

McDonald, I.K., and Thornton, J.M. (1994). Satisfying hydrogen bonding potential in proteins. J. Mol. Biol. *238*, 777–793.

McRee, D.E. (1993). Practical Protein Crystallography (San Diego: Academic Press, Inc).

Momburg, F., Roelse, J., Howard, J.C., Butcher, G.W., Hämmerling, G.J., and Neefjes, J.J. (1994). Selectivity of MHC-encoded peptide transporters from human, mouse and rat. Nature *367*, 648–651.

Navaza, J. (1994). AMoRe: an automated package for molecular replacement. Acta Crystallogr. A *50*, 157–163.

Nicholls, A., Sharp, K.A., and Honig, B. (1991). Protein folding and association: insights from the interfacial and thermodynamic properties of hydrocarbons. Proteins *11*, 281–296.

Otwinowski, Z., and Minor, W. (1997). Processing of x-ray diffraction data collected in oscillation mode. Methods Enzymol. *276*, 307–326.

Powis, S.J., Deverson, E.V., Coadwell, W.J., Ciruela, A., Huskisson, N.S., Smith, H., Butcher, G.W., and Howard, J.C. (1992). Effect of polymorphism of an MHC-linked transporter on the peptides assembled in a class I molecule. Nature *357*, 211–215.

Powis, S.J., Young, L.L., Joly, E., Barker, P.J., Richardson, L., Brandt, R.P., Melief, C.J., Howard, J.C., and Butcher, G.W. (1996). The rat *cim* effect: TAP allele-dependent changes in a class I MHC anchor motif and evidence against C-terminal trimming of peptides in the ER. Immunity *4*, 159–165.

Read, R.J. (1986). Improved fourier coefficients for maps using phases from partial structures with errors. Acta Crystallogr. A *42*, 140–149.

Reiser, J., Darnault, C., Guimezanes, A., Grégoire, C., Mosser, T., Schmitt-Verhulst, A., Fontecilla-Camps, J.C., Malissen, B., Housset, D., and Mazza, G. (2000). Crystal structure of a T cell receptor bound to an allogenic MHC molecule. Nat. Immunol. *1*, 291–297.

Rognan, D., Scapozza, L., Folkers, G., and Daser, A. (1994). Molecular dynamics simulation of MHC-peptide complexes as a tool for predicting potential T cell epitopes. Biochemistry *33*, 11476–11485.

Saito, N.G., Chang, H.C., and Paterson, Y. (1999). Recognition of an MHC class I-restricted antigenic peptide can be modulated by para-substitution of its buried tyrosine residues in a TCR-specific manner. J. Immunol. *162*, 5998–6008.

Schmitt, L., Boniface, J.J., Davis, M.M., and McConnell, H.M. (1999). Conformational isomers of a class II MHC-peptide complex in solution. J. Mol. Biol. *286*, 207–218.

Sheriff, S., Hendrickson, W.A., and Smith, J.L. (1987). Structure of myohemerythrin in the azidomet state at 1.7/1.3 Å resolution. J. Mol. Biol. *197*, 273–296.

Speir, J.A., Garcia, K.C., Brunmark, A., Degano, M., Peterson, P.A., Teyton, L., and Wilson, I.A. (1998). Structural basis of 2C TCR allorecognition of H-2L^{d} peptide complexes. Immunity *8*, 553–562.

Speir, J.A., Abdel-Motal, U.M., Jondal, M., and Wilson, I.A. (1999). Crystal structure of an MHC class I presented glycopeptide that generates carbohydrate-specific CTL. Immunity *10*, 51–61.

Stevens, J., Wiesmüller, K.-H., Barker, P.J., Walden, P., Butcher, G.W., and Joly, E. (1998a). Efficient generation of major histocompatibility complex class I-peptide complexes using synthetic peptide libraries. J. Biol. Chem. *273*, 2874–2884.

Stevens, J., Wiesmüller, K.-H., Walden, P., and Joly, E. (1998b). Peptide length preferences for rat and mouse MHC class I molecules using random peptide libraries. Eur. J. Immunol. *28*, 1272–1279.

Stevens, J., Jones, R.C., Bordoli, R.S., Trowsdale, J., Gaskell, S.J., Butcher, G.W., and Joly, E. (2000a). Peptide specificity of RT1-A1^{c}, an inhibitory rat major histocompatibility complex class I natural killer cell ligand. J. Biol. Chem. *275*, 29217–29224.

Stevens, J., Wiesmüller, K.-H., Butcher, G.W., and Joly, E. (2000b). Analysis of peptide length preference of the rat MHC class Ia molecule RT1-A^{u}, by a modified random peptide library approach. Int. Immunol. *12*, 83–89.

Thorpe, C.J., Moss, D.S., Powis, S.J., Howard, J.C., Butcher, G.W., and Travers, P.J. (1995). An analysis of the antigen-binding site of RT1-A^{a} suggests an allele-specific motif. Immunogenetics *41*, 329–331.

Viner, N.J., Nelson, C.A., Deck, B., and Unanue, E.R. (1996). Complexes generated by the binding of free peptides to class II MHC molecules are antigenically diverse compared with those generated by intracellular processing. J. Immunol. *156*, 2365–2368.

Willcox, B.E., Gao, G.F., Wyer, J.R., Ladbury, J.E., Bell, J.I., Jakobsen, B.K., and van der Merwe, P.A. (1999). TCR binding to peptide-MHC stabilizes a flexible recognition interface. Immunity *10*, 357–365.

Wilson, I.A. (1999). Class-conscious TCR? Science *286*, 1867–1868.

Wilson, I.A., and Stanfield, R.L. (1993). Antibody-antigen interactions. Curr. Opin. Struct. Biol. *3*, 113–118.

Wilson, I.A., and Stanfield, R.L. (1994). Antibody-antigen interactions: new structures and new conformational changes. Curr. Opin. Struct. Biol. *4*, 857–867.

Young, A.C., Zhang, W., Sacchettini, J.C., and Nathenson, S.G. (1994). The three-dimensional structure of H-2D^{b} at 2.4 Å resolution: implications for antigen-determinant selection. Cell *76*, 39–50.

Zeng, Z., Castaño, A.R., Segelke, B.W., Stura, E.A., Peterson, P.A., and Wilson, I.A. (1997). Crystal structure of mouse CD1: an MHC-like fold with a large hydrophobic binding groove. Science *277*, 339–345.

Protein Data Bank ID Code

Coordinates and structure factors for the RT1-A^{a}-MTF-E complexes have been deposited in the Protein Data Bank under ID code 1ED3.